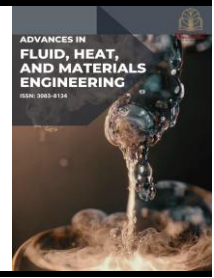




Advances in Fluid, Heat and Materials Engineering

Journal homepage:
<https://karyailham.com.my/index.php/afhme/index>
ISSN: 3083-8134



Computational Modelling of Flow Characteristic in a Venturi Flow

Muhamad Yusra Habil Yusri¹, Ishkrizat Taib^{1,*}

¹ Department of Mechanical Engineering, Faculty of Mechanical and Manufacturing Engineering, Universiti Tun Hussein Onn Malaysia, 86400 Parit Raja, Johor, Malaysia

ARTICLE INFO

Article history:

Received 25 April 2026
Received in revised form 10 May 2026
Accepted 3 June 2026
Available online 30 June 2026

Keywords:

Bernoulli; ANSYS Fluent; grit independence test; pressure drop; velocity distribution

ABSTRACT

The Venturi flow meter is widely used in fluid engineering applications to measure the flowrate of liquids and gases due to its simple design and low-pressure loss. However, the accuracy of pressure prediction in Computational Fluid Dynamics (CFD) simulations can be influenced by the turbulence model selected which may lead to variations of the simulation results. Therefore, this study investigates the pressure characteristics of a Venturi flow meter and compares the performance of three turbulence models using Ansys Fluent. A three-dimensional Venturi flow meter with inlet and outlet diameters of 30mm, a throat with diameter of 15mm and a total length of 185mm was developed and analysed under steady state conditions. Water was used as the working fluid with an inlet velocity of 2.2 m/s. To ensure reliable numerical results, a Grid Independence Test (GIT) was conducted and a mesh with an element size of 3.5mm consisting of 17962 nodes and 13584 elements was selected for the final simulation. Three turbulence models were evaluated which realizable $k-\epsilon$ models, the standard $k-\epsilon$ and standard $k-\omega$. The results showed a pressure drop of approximately 8397.8 Pa between the inlet and throat sections followed by pressure recovery towards the outlet which agrees with the operating principle of the venturi flow meter. All three turbulence models were able to predict the general pressure and velocity behaviour within the flow domain. However, differences were observed in their convergence performance and flow predictions. Among these models tested, the most stable convergence behaviour is the realizable $k-\epsilon$ models and produced smoother pressure contours and velocity streamlines compared to the others model. Based on the findings, the realizable $k-\epsilon$ models was identified as the most suitable turbulence model for predicting the pressure characteristics of the venturi flow meter.

1. Introduction

Fluid flow measurement is important aspect in engineering study or industry especially in piping system involving liquid and gas transportation. To ensure efficiency of system performance, energy conservation and process control in industries which accurate measurement of flow rate and pressure variation is necessary. This is related to our case study which among the various flow measuring devices available, the venturi Flow meter is commonly recognized as one of the accurate

* Corresponding author.

E-mail address: iszat@uthm.edu.my

<https://doi.org/10.37934/afhme.9.1.1018a>

differential pressures due to its simple design and stable operating performance [1]. This study conducted to study the pressure distribution inside a venturi flow meter using CFD simulation. Besides that, to compare three turbulence models which are standard $k-\epsilon$, standard $k-\omega$, and realizable $k-\epsilon$.

The venturi flow meter operates based on Bernoulli's principle where a fluid flowing through converging section experiences as increase in velocity and decrease in static pressure at the throat section. The pressure difference between the inlet and throat is used to determine the flowrate [2]. Because of this relationship, the pressure characteristic involved inside the venturi meter is key factor in evaluating its performance and accuracy.

In real engineering systems, fluid flow inside a venturi meter is usually turbulent because of its high velocity and sudden change. This makes the flow difficult to study using experiments alone since pressure and velocity are always changing. This is how CFD workflow help to simulate this kind of flow because it can show pressure and velocity behaviour without doing any physical testing [3]. However, CFD results depend strongly on the turbulence model used. Different models such as standard $k-\epsilon$, standard $k-\omega$, and realizable $k-\epsilon$ may give different pressure predictions even when using the same geometry and boundary conditions [4].

Therefore, selecting on appropriate turbulence model is essential to obtain reliable pressure predictions in CFD simulations. Previous studies have shown that different turbulence models may perform differently depending on flow condition, geometry and pressure gradient involved in the system. The accuracy of the turbulence model becomes an important factor in predicting the pressure distribution within flow domain [5]. This study aims to analyse the pressure characteristics of a Venturi flow meter using CFD simulation and compare the performance of three commonly used turbulence models which are standard $k-\epsilon$, Standard $k-\omega$, and Realizable $k-\epsilon$. The findings of this study are expected to provide a better understanding of the influence of turbulence model selection on pressure prediction and flow behaviour within a Venturi flow meter.

2. Methodology

This study investigates the pressure characteristics of a Venturi flow meter using Computational Fluid Dynamics (CFD) simulation through ANSYS Design Modeler and Ansys Fluent software. CFD was chosen because it offers a cost effective and efficient way to analyze fluid behavior inside the Venturi meter without the need for physical experimental setups. By using CFD, it is possible to visualize and analyze the pressure distribution along the venturi meter in detail including regions that would be difficult to measure experimentally such as the throat section where the pressure drop is most significant. The methodology includes the geometry creation of the Venturi flow meter, mesh generation, specification of boundary conditions, selection of turbulence models, governing equation, solver setup and Grid Independence Test (GIT).

2.1 Geometry of Venturi Flow Meter

The geometry used in this study is a venturi flow meter which is a device that consist of three main sections as converging inlet, throat section and diverging outlet. As in Figures 1(a), (b) and Table 1 clearly show the geometry dimensions and 3d layout of the case study venturi meter. The converging and diverging sections were designed to provide smooth flow acceleration and pressure recovery. After defining the dimensions, the venturi flow meter was developed in ANSYS Design Modeler as a three-dimensional solid model by using revolve tool with specific axis selected and the final geometry is shown in Figure 1(b).

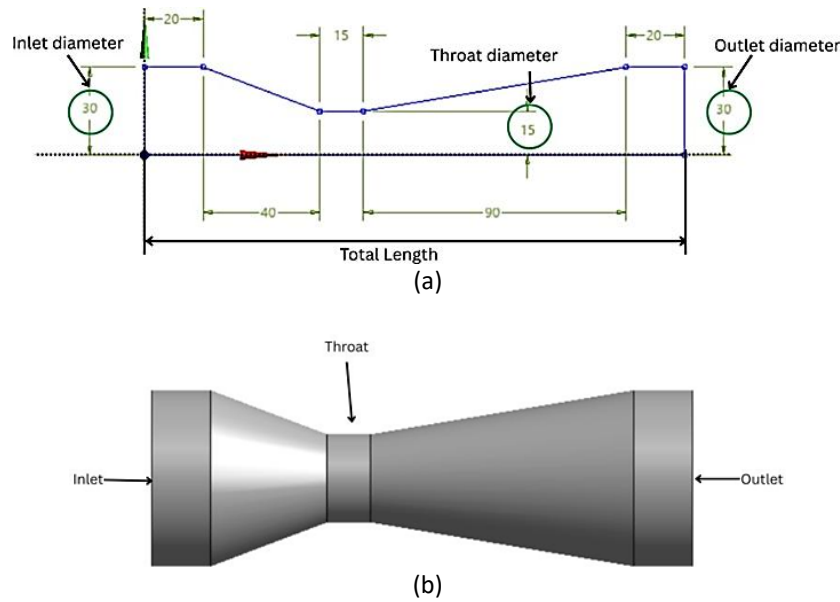


Fig. 1. Figure of Venturi meter (a) Venturi meter’s dimensions (b) 3D layout of venturi meter

Table 1

The dimensions of the mercury meter

Parameter	Value
Inlet diameter	30 mm
Throat diameter	15 mm
Outlet diameter	30 mm
Total length	185 mm
Working fluid	Water, H ₂ O

2.2 Mesh Generation

Meshing is an important step in CFD simulation because the fluid domain needs to be divided into many small elements before the governing equations can be solved. In a Venturi flow meter, the fluid experiences a significant change in velocity and pressure, especially at the throat section. Therefore, a suitable mesh is needed to capture these changes and obtain reliable results [6]. After the venturi flow meter was created, it was transferred to ANSYS Meshing for mesh generation. In this study, the mesh was generated by default meshing setting which is unstructured tetrahedral mesh. A global element size of 3.5mm was used throughout the geometry. The generated mesh consisted of 17962 nodes and 13584 elements. Named selection were also created as inlet, outlet and wall surfaces as shown in Figure 2 to make the boundary condition setup easier and clear in ANSYS Fluent.

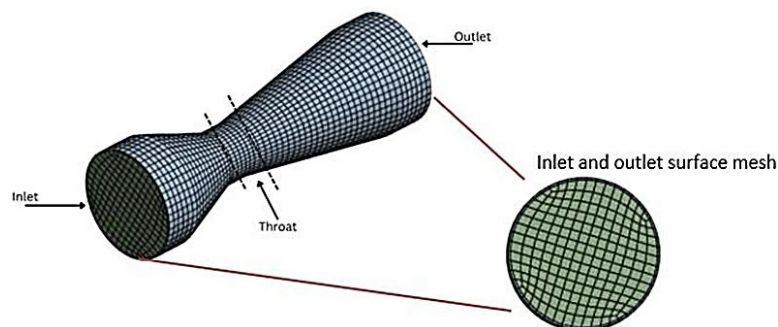


Fig. 2. Mesh generation of the venturi flow meter

2.3 Boundary Conditions

After the meshing was completed, the model was imported into ANSYS Fluent for simulation. The named selections created during the meshing stage were automatically recognized as inlet, outlet and wall boundaries. In other hand, water liquid (H_2O) was selected as the material of working fluid for this study because it is one of commonly used fluids in piping industry and flow measurement applications [7,15]. The Figure 3 below is showing the boundary condition setup which a velocity inlet of 2.2 m/s was assigned at the inlet section, while a pressure outlet with a gauge pressure of 0 Pa was specified at the outlet. The fluid enters from inlet through the converging section and accelerates towards the throat. As the flow passes through the diffuser section, the velocity decreases and the pressure recovers [8-11].

Although the geometry, fluid properties, inlet velocity and pressure outlet settings were kept constant, different turbulence models were applied to investigate their effect on pressure characteristics which are standard $k-\epsilon$, realizable $k-\epsilon$ and standard $k-\omega$ models. These models were chosen because they are the most commonly used turbulence models in engineering CFD applications. The Standard $k-\epsilon$ model is widely used for general-purpose flow simulations, while the Realizable $k-\epsilon$ model provides improved predictions for flows involving strong pressure gradients. The Standard $k-\omega$ model is known for its ability to capture near-wall flow behaviour more accurately [6,12,13]. These boundary conditions were selected to simulate the flow behaviour within the venturi flow meter under steady state conditions.

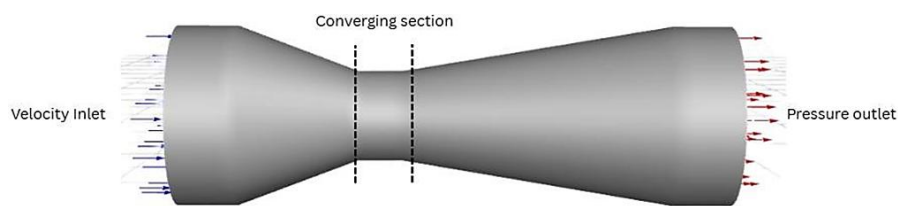


Fig. 3. Boundary conditions setup for the Venturi flow meter

2.4 Governing Equations on Venturi Flow Meter

The flow inside a venturi flow meter can be explained by using several basic fluid mechanics equations. In this study, Bernoulli's principle and the continuity equation are used to describe the relationship between pressure, velocity and flow area. These equations help explain the pressure drop at the throat section and support the analysis of the CFD simulation results.

2.4.1 Continuity equation

The continuity equation is based on the conservation of mass, which states that the amount of fluid entering the system must be equal to the amount of leaving the system. As the flow area decreases, the fluid velocity increases to maintain a constant flow rate as written in Eq. (1):

$$\nabla \cdot \vec{V} \rightarrow = 0 \quad (1)$$

where $\vec{V} \rightarrow$ is velocity vector.

2.4.2 Momentum equation and Bernoulli's principle

The momentum equation is used to determine the pressure and velocity distribution within the fluid domain. In ANSYS Fluent, the momentum equation is solved numerically together with the selected turbulence model to predict the flow behaviour inside the Venturi flow meter as written in Eq. (2):

$$\rho(\vec{V} \rightarrow \cdot \nabla) \vec{V} \rightarrow = -\nabla p + \mu \nabla^2 \vec{V} \rightarrow \quad (2)$$

where (ρ) is fluid density, (p) is pressure and (μ) is dynamic viscosity. Bernoulli's principle is used to explain the relationship between pressure and velocity within the Venturi flow meter [10]. As the flow passes through the throat section, the reduction in flow area causes the velocity to increase and the static pressure to decrease, the principle is written as below in Eq. (3) [14-16]:

$$P + \frac{1}{2}\rho V^2 + \rho gh = \text{constant} \quad (3)$$

where (P) is the static pressure, (ρ) is the fluid density, (V) is the fluid velocity, (g) is the gravitational acceleration and (h) is the elevation height.

2.5 Solver Setup

After the boundary conditions were assigned and different turbulence models were selected, the solver settings were adjusted in ANSYS Fluent. In this study, the Semi-Implicit Method for Pressure-Linked Equations (SIMPLE) scheme was used for pressure-velocity coupling to obtain stable convergence during the simulation. The solution was initialized by using the Hybrid Initialization method with the inlet boundary selected as the region. The same solver settings were applied to all turbulence models to ensure a fair comparison of the simulation results.

2.6 Grid Independence Test

A Grid Independence Test (GIT) was conducted to ensure that the CFD results were not significantly affected by the mesh density used in the simulation. In CFD analysis, the mesh is crucial part in determining the accuracy of the numerical solution. A very coarse mesh may not accurately capture the flow behaviour, while fine mesh can increase computational time without doing significant improvement in the results [17-20]. Therefore, a grid independence test was performed before the final simulations.

In this study, three different mesh elements sizes were evaluated which is 3.5 mm, 2.0 mm and 1.0 mm. For each mesh size, the same geometry as well as fluid properties, inlet velocity, boundary conditions and solver settings were maintained to ensure a fair comparison. The inlet pressure and throat pressure were selected as the monitoring parameters because the pressure difference between these locations represents the main operating characteristics of the venturi flow meter. The pressure values obtained from each mesh were recorded and compared to determine the influence of mesh density on the numerical solution.

3. Results

3.1 Grid Independence Test's Analysis

Table 2 shows the results of the Grid Independence Test (GIT) conducted using three different mesh step which named as coarse, medium and fine. From the table, it can be observed that the predicted pressure drop increases from 8397.8 Pa to 8590.3 Pa as the mesh becomes finer as shown in Figure 4 below. This indicates that the mesh is able to capture the pressure variation within the Venturi flow meter more accurately. The difference in pressure drop between the medium and fine meshes was relatively small with an increase of only 43.8 Pa. This suggests that the numerical solution is approaching an independent mesh condition where further mesh adjustment would have limited effect. In addition, the inlet and throat pressure values showed a consistent trend as the mesh became finer which indicate the stable numerical result. The grid independence test confirms that the selected mesh is sufficient for comparing the pressure characteristics of different turbulence models in the venturi flow meter simulation.

Table 2
 Grid independence test results

Design point	Mesh type	Mesh element size	Inlet pressure	Throat pressure	Pressure drop
Dp 0	Coarse	3.5	5764.2	-2633.6	8397.8
Dp 1	Medium	2.0	5841.7	-2704.8	8546.5
Dp 2	Fine	1.0	5868.9	-2721.4	8590.3

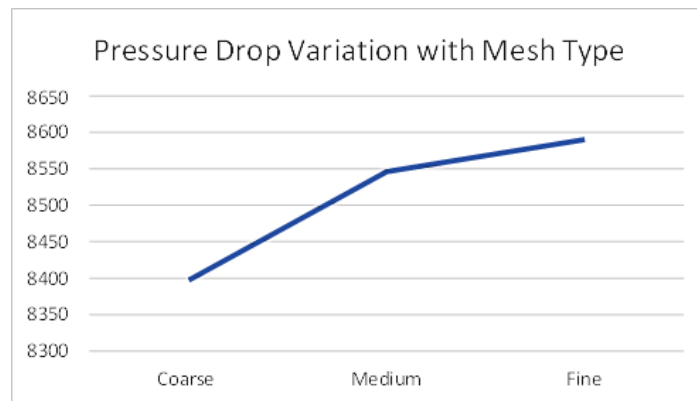


Fig. 4. Pressure drop variation with mesh type

3.2 Pressure Distribution

The pressure contours obtained for each turbulence model are presented in Figure 5(a), Figure 5(b) and Figure 5(c). All turbulence models show a similar pressure distribution pattern, where the highest pressure occurs at the inlet section, followed by a significant pressure drop at the throat and gradual pressure recovery at the outlet. This behaviour is consistent with the venturi effect and bernoulli's principle which state that an increase in fluid velocity results in a reduction in static pressure. As the fluid passes through the converging section, the flow area decreases causing the velocity to increase rapidly until its reached maximum value at the throat.

Among the three turbulence models, the realizable k-ε model produces the smoothest pressure gradient and the most uniform pressure recovery throughout the domain. This explained that the model is better to capture the pressure variation along with the acceleration of the fluid inside the venturi meter. The standard k-ε model predicts similar pressure distribution but shows slightly less

uniform contour near the throat region. In comparison, the standard $k-\omega$ model show more irregular pressure contours at the expansion sections which explained a higher sensitivity to flow changes and pressure gradients. Nevertheless, all three models successfully captured the expected pressure characteristics of the venturi flow meter.

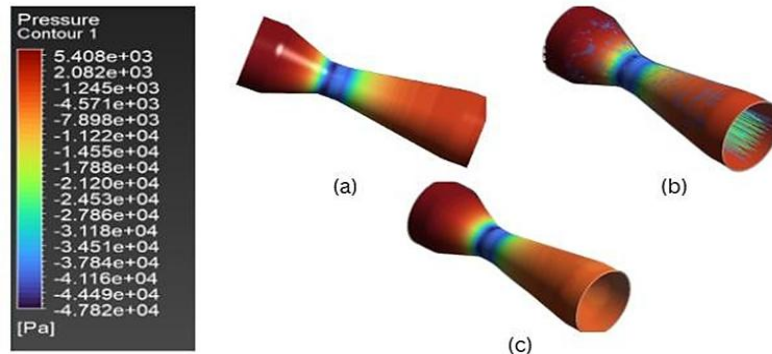


Fig. 5. Pressure contour for 5(a) $k-\epsilon$ realizable, 5 (b) $k-\epsilon$ standard and 5 (c) $k-\omega$

3.3 Velocity Distribution

The velocity Streamline plots are shown in Figure 6. The fluid velocity increases as it enters the throat section and decreases again towards the outlet. This happens because the throat has the smallest flow area causing the fluid to accelerate as it passes through the region. The highest velocity can be seen at the throat while lower velocities are observed at the inlet and outlet sections. Overall, the three turbulence models predict a similar flow pattern. However, the realizable $k-\epsilon$ model shows a smoother flow distribution from the inlet to the outlet. The standard $k-\epsilon$ model gives almost the same behaviour, although the streamlines appear slightly less uniform near the throat section.

For the standard $k-\omega$ model, the streamlines show more variation, especially near the wall region and diffuser section. This indicates that the model is more sensitive to changes in the flow near the wall. The maximum velocity predicted by all three models is approximately 9.8 m/s. This suggests that the geometry and boundary conditions have a greater influence on the velocity increase than the choice of turbulence model. Based on the streamline distribution, the realizable $k-\epsilon$ model provides the most consistent flow pattern among the three models investigated in this study.

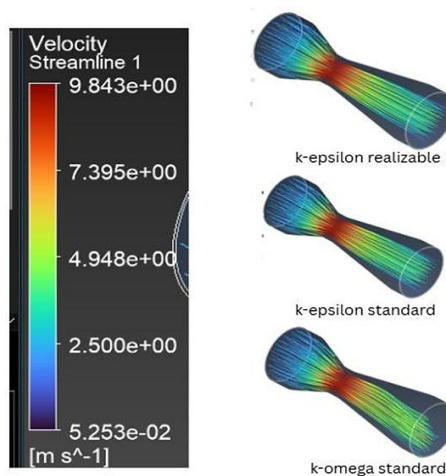


Fig. 6. Velocity Streamline for 7(a) $k-\epsilon$ realizable 7(b) $k-\epsilon$ standard 7(c) $k-\omega$

4. Conclusions

This study investigated the pressure characteristics of a Venturi flow meter using Computational Fluid Dynamic (CFD) simulation in ANSYS fluent. A Grid independence Test (GIT) was conducted to ensure that the numerical results were not significantly affected by the mesh size. The selected mesh was then used to compare the performance of three turbulence models which are standard k- ϵ , realizable k- ϵ and standard k- ω models.

The pressure contour results showed that all turbulence models successfully predicted a pressure drop at the throat section followed by recovery at the outlet. The velocity streamline results also showed that the fluid velocity increased significantly at the throat due to the reduction in flow area and decreased again in the diffuser section. The maximum velocity predicted by all three models was approximately 9.8 m/s.

Although the overall flow pattern was kind similar for all turbulence models, slight differences were observed in the pressure and velocity distribution. Among the models investigated, the realizable k- ϵ model produced the smoothest pressure contours and most uniform streamline distribution. In conclusion, it was the most suitable model for predicting the pressure characteristics of the venturi flow meter in this study. Overall, the objectives of the study were successfully achieved through the comparison of turbulence models and the analysis of pressure and velocity behaviour inside the venturi flow meter.

References

- [1] Akpan, P. U. "A cfd simulation of water flow through a variable area venturi meter." *International Journal of Current Research* 6 6 (2014): 5425-5431.
- [2] Baylar, Ahmet, M. Cihan Aydin, Mehmet Unsal, and Fahri Ozkan. "Numerical modeling of venturi flows for determining air injection rates using FLUENT V6. 2." *Mathematical and Computational Applications* 14, no. 2 (2009): 97. <https://doi.org/10.3390/mca14020097>
- [3] Shi, Hongbo, Mingda Li, Petr Nikrityuk, and Qingxia Liu. "Experimental and numerical study of cavitation flows in venturi tubes: From CFD to an empirical model." *Chemical Engineering Science* 207 (2019): 672-687. <https://doi.org/10.1016/j.ces.2019.07.004>
- [4] Fletcher, David F., Vishal Chaugule, Larissa Gomes dos Reis, Paul M. Young, Daniela Traini, and Julio Soria. "On the use of computational fluid dynamics (CFD) modelling to design improved dry powder inhalers: Fletcher et al." *Pharmaceutical research* 38, no. 2 (2021): 277-288. <https://doi.org/10.1007/s11095-020-02981-y>
- [5] Tomaszewska-Wach, Barbara, and Grzegorz Ligus. "Assessment of the impact of k- ϵ and k- ω turbulence models on the compatibility of CFD simulations with PIV measurements for flow through a measuring orifice." *Applied Sciences* 15, no. 22 (2025): 12204. <https://doi.org/10.3390/app152212204>
- [6] Moukalled, Fadl, Luca Mangani, and Marwan Darwish. "The finite volume method." In *The finite volume method in computational fluid dynamics: An advanced introduction with OpenFOAM® and Matlab*, pp. 103-135. Cham: Springer International Publishing, 2015. https://doi.org/10.1007/978-3-319-16874-6_5
- [7] Launder, Brian Edward, and Dudley Brian Spalding. "The numerical computation of turbulent flows." In *Numerical Prediction of Flow, Heat Transfer, Turbulence and Combustion*, pp. 96-116. Pergamon, 1983. <https://doi.org/10.1016/B978-0-08-030937-8.50016-7>
- [8] Ghaderi, Amir, Amir Hossein Rezaei, Fatemeh Nazari, and Hossein Mohammadnezhad. "Numerical investigation of the impact of hydraulic behavior of various constrictions on a venturi channel." *Results in Engineering* (2025): 106916. <https://doi.org/10.1016/j.rineng.2025.106916>
- [9] Song, Hongqing. *Engineering fluid mechanics*. Vol. 2024. Singapore: Springer, 2018. <https://doi.org/10.1007/978-981-13-0173-5>
- [10] Nakayama, Yasuki. *Introduction to fluid mechanics*. Butterworth-Heinemann, 2018. <https://doi.org/10.1016/B978-0-08-102437-9.00001-2>
- [11] Çengel, Yunus A., and John M. Cimbala. *Fluid mechanics: Fundamentals and applications*. McGraw Hill, 2024.
- [12] Wilcox, David C. *Turbulence modeling for CFD*. Vol. 2. La Canada, CA: DCW industries, 1998.

- [13] Shih, Tsan-Hsing, William W. Liou, Aamir Shabbir, Zhigang Yang, and Jiang Zhu. "A new k- ϵ eddy viscosity model for high reynolds number turbulent flows." *Computers & fluids* 24, no. 3 (1995): 227-238. [https://doi.org/10.1016/0045-7930\(94\)00032-T](https://doi.org/10.1016/0045-7930(94)00032-T)
- [14] Zhan, Mengke, Muhammad Alif Bin Razali, Ayush Moitra, Cheng-Gang Xie, Wai Lam Loh, and Jian-Jun Shu. "Influence of design parameters of upstream Venturi pipeline on multiphase flow measurement." *Engineering Applications of Computational Fluid Mechanics* 17, no. 1 (2023): 2182831. <https://doi.org/10.1080/19942060.2023.2182831>
- [15] Diaz, Diego del Olmo, and Denis F. Hinz. "Performance of eddy-viscosity turbulence models for predicting swirling pipe-flow: Simulations and laser-Doppler velocimetry." *arXiv preprint arXiv:1507.04648* (2015).
- [16] Zhang, J. X. "Analysis on the effect of venturi tube structural parameters on fluid flow." *AIP Advances* 7, no. 6 (2017). <https://doi.org/10.1063/1.4991441>
- [17] Fadaei, Mehdi, Forough Ameli, and Seyed Hasan Hashemabadi. "Experimental study and CFD simulation of two-phase flow measurement using orifice flow meter." (2019): 85-96.
- [18] Gümüşel, Hasan Tolg. "Numerical investigation of cavitating flow in variable area venturi on the basis of experimental data." Master's thesis, Middle East Technical University (Turkey), 2020.
- [19] Campana, Patrick L. "Application of Computational Fluid Dynamics to Determine Gas Expansion Factors of Differential Pressure Flow Meters." Master's thesis, Utah State University, 2021.
- [20] Jiao, Zun, You Chen, and Chunwei Lyu. "Factors correlated with personal growth initiative among college students: A meta-analysis." *Heliyon* 10, no. 7 (2024). <https://doi.org/10.1016/j.heliyon.2024.e28518>